Universal quantum computing with spin and valley states

2012 New J. Phys. 14 083008

(http://iopscience.iop.org/1367-2630/14/8/083008)

New Journal of Physics
The open-access journal for physics

Universal quantum computing with spin and valley states

Niklas Rohling and Guido Burkard[1]
Department of Physics, University of Konstanz, D-78457 Konstanz, Germany
E-mail: Guido.Burkard@uni-konstanz.de

New Journal of Physics **14** (2012) 083008 (19pp)
Received 22 March 2012
Published 10 August 2012
Online at http://www.njp.org/
doi:10.1088/1367-2630/14/8/083008

Abstract. We investigate a two-electron double quantum dot with both spin and valley degrees of freedom as they occur in graphene, carbon nanotubes or silicon and regard the 16-dimensional space with one electron per dot as a four-qubit logic space. In the spin-only case, it is well known that the exchange coupling between the dots combined with arbitrary single-qubit operations is sufficient for universal quantum computation. The presence of valley degeneracy in the electronic band structure alters the form of the exchange coupling and, in general, leads to spin–valley entanglement. Here, we show that universal quantum computation can still be performed by exchange interaction and single-qubit gates in the presence of an additional (valley) degree of freedom. We present an explicit pulse sequence for a spin-only controlled-NOT consisting of the generalized exchange coupling and single-electron spin and valley rotations. We also propose state preparations and projective measurements with the use of adiabatic transitions between states with (1,1) and (0,2) charge distributions similar to the spin-only case, but with the additional requirement of controlling the spin and valley Zeeman energies by an external magnetic field. Finally, we demonstrate a universal two-qubit gate between a spin and a valley qubit, allowing universal gate operations on the combined spin and valley quantum register.

[1] Author to whom any correspondence should be addressed.

Contents

1. Introduction

Since Loss and DiVincenzo [1] proposed quantum computing with electron spins in double quantum dots, there has been substantial experimental progress in the field of coherent spin manipulation in semiconductors [2–6]. The majority of these experiments have been performed in gallium arsenide (GaAs), where the electron spin is affected by decoherence due to its coupling to a typically large number of nuclear spins, as well as spin relaxation due to spin–orbit coupling.

In carbon materials such as graphene or carbon nanotubes (CNTs), the hyperfine interaction is much weaker, because ^{13}C is the only naturally occurring carbon isotope carrying a nuclear spin and the amount of ^{13}C in natural carbon is merely $\sim$1%. Similar considerations hold for quantum dots based on silicon (Si) and germanium (Ge), where less than 5% (8%) of all naturally occurring Si (Ge) atoms carry a nuclear spin. In graphene, the spin–orbit coupling is also expected to be weak [7].

However, the situation for quantum dots in graphene and CNTs compared to GaAs is complicated by the presence of an additional orbital degree of freedom, the so-called valley iso-spin [7, 8], with basis states $|K\rangle$ and $|K'\rangle$ denoting the two inequivalent Dirac points in the first Brillouin zone in the graphene band structure. Experimentally, spin states in graphene quantum dots have been identified by transport measurements [9] but valley states have not yet been observed, whereas in CNTs, a fourfold grouping of electronic states due to spin and valley degrees of freedom has already been observed for a decade in transport measurements [10–12]. The relaxation and dephasing times of two valley- and spin-degenerate electrons in a CNT double quantum dot have been studied experimentally [13] by using both transport measurements in the Pauli blockade regime [14] and pulsed-gate measurements [15, 16].

Interestingly, the situation for quantum dots in two-dimensional silicon structures such as Si/SiGe heterostructures or Si/metal oxide semiconductors is similar since the sixfold

valley degeneracy in bulk silicon is partially lifted in strained systems [17, 18], giving rise to the remaining twofold valley degeneracy. The confining potential can lead to a further splitting of the remaining two valley states, which ultimately leads back to spin-only qubits and operations [19]. In recent experiments with silicon-based quantum dots, coherent spin manipulation with the exchange interaction has been performed successfully [20]. Some control over the valley splitting has been demonstrated by conduction measurements [21]. A dependence of the valley splitting on electric fields has been predicted [22] and is a possible reason for the different valley splittings measured in recent experiments [23, 24]. Another material with valley degeneracy is AlAs, where the control of valley splitting by tunable strain has been demonstrated [25, 26]. For Si [27] and graphene [8, 28, 29] as well as for AlAs [30, 31], there have been speculations that the valley degree of freedom might serve as an additional resource for classical or quantum information processing, i.e. as a classical bit for valleytronics [8, 28, 30] or as a qubit [27, 29, 31]. However, the presence of an orbital (e.g. valley) degeneracy leads to the following difficulty in quantum computing. The additional degree of freedom modifies the form of the exchange interaction which is based on the Pauli exclusion principle. For example, a spin triplet in the (1,1) charge configuration may not be blocked from tunneling to a (0,2) state if the two electrons reside in different valleys. Here, (m,n) stands for m electrons in the left and n electrons in the right quantum dot. Such a valley-dependent spin exchange leads to spin–valley entanglement and implies that the controlled-NOT (CNOT) gate cannot be performed in the same way as proposed in [1] as long as valley degeneracy is present [8].

Therefore, proposals for graphene quantum dots have tried to avoid valley degeneracy [7] by using the armchair boundary condition for quantum dots in a graphene nanoribbon [8] or by applying a magnetic field perpendicular to the graphene sheet for quantum dots defined by electrostatic gates [32]. In a recent proposal, Wu *et al* [33] suggest using only the valley degree of freedom as a qubit and fix the spin degree of freedom by a strong in-plane magnetic field. Also, for Si quantum dots, the possibilities of valley-only qubit manipulation are currently under theoretical investigation [34–36].

In this paper, we consider a double quantum dot with two electrons and regard both spin and valley degrees of freedom as potential qubits. This leads to a 16-dimensional logic space consisting of two spin and two valley qubits (see figure 1). We show that it is possible to perform a CNOT gate as a universal two-qubit gate exclusively on the spin or the valley qubits if the exchange interaction and single-qubit manipulations can be implemented. For singlet–triplet qubits the exchange interaction directly produces a CNOT gate, up to single-qubit operations. Furthermore, we investigate how state preparation and measurements can be carried out by adiabatically changing the asymmetry between the dots with the use of the appropriate gate voltage control. An external magnetic field turns out to be important for both preparation and measurement. The field allows one to break the sixfold degeneracy of the states with both electrons in the same dot, (2,0) and (0,2), and thus allows for the selective preparation of one such state in the initialization process. The magnetic field also selects the states that are driven from a symmetric (1,1) back to this asymmetric (2,0) or (0,2) charge state. For quantum state readout, the resulting charge state can then be measured with a charge detector, e.g. a nearby quantum point contact [6]. We explain below how a projective measurement on one specific state can be achieved by three charge measurements under different configurations of the magnetic field or, alternatively, with a constant magnetic field and with the help of single-qubit operations.

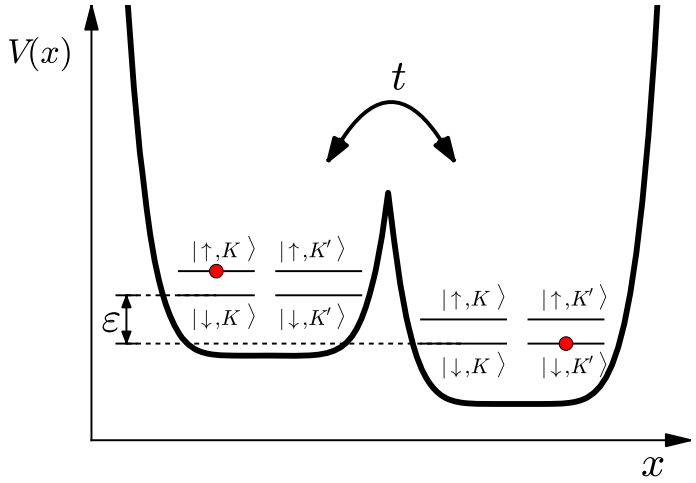

Figure 1. Schematic representation of a double quantum dot formed by a confinement potential $V(x)$ and filled with two electrons (red dots). In the presence of valley and spin degeneracy there are 16 states with one electron in each dot, i.e. in the (1,1) charge configuration. In the example shown here, the two-electron state is $|s_1, s_2, \tau_1, \tau_2\rangle = |\uparrow, \downarrow, K, K'\rangle$. The hopping (tunneling) matrix element between the dots and the inter-dot bias energy are denoted by t and ε.

This paper is organized as follows. In section 2, we introduce the model Hamiltonian for the tunnel-coupled double quantum dot with two electrons, and derive the general form of the exchange interaction without a magnetic field (section 2.1) and with a magnetic field (section 2.2). Section 3 contains a pulse sequence for the CNOT gate. Our considerations and results concerning state preparation and measurement are reported in section 4. In section 5, we describe how a quantum register using spin and valley qubits may be constructed using singlet–triplet qubits in two quantum dots and usual single-electron spin and valley qubits in the other dots. Conclusions are drawn and an outlook towards possible further investigations is given in section 6.

2. The model

We consider two electrons in a double quantum dot described by the Hamiltonian

$$H = H_0 + H_T + H_B, \tag{1}$$

where the two quantum dots with one orbital each are described by

$$H_0 = \frac{\varepsilon}{2}(\hat{n}_1 - \hat{n}_2) + U \sum_{j=1,2} \hat{n}_j(\hat{n}_j - 1), \tag{2}$$

with ε denoting the difference between the energy levels of the two dots, controllable by gate voltages (figure 1). The additional Coulomb energy of two electrons in the same dot is denoted by U. The number operators $\hat{n}_j$ $(j = 1, 2)$ include a sum over the spin $s = \uparrow, \downarrow$ and the valley degree of freedom $\tau = \pm \equiv K, K'$,

$$\hat{n}_j = \sum_{s,\tau} \hat{c}^\dagger_{js\tau} \hat{c}_{js\tau}, \tag{3}$$

where $\hat{c}^{(\dagger)}_{j,s\tau}$ annihilates (creates) an electron in the jth quantum dot with spin and valley quantum numbers s and τ. In the spin-only case, the Hilbert space for this model of a double quantum dot consists of four states with a (1,1) charge distribution, one (0,2) and one (2,0) charge state [1], where (n,m) denotes a state with n electrons in the left and m electrons in the right dot. No further states with two electrons in one dot with a single orbital are permitted by the Pauli principle. Including the valley degree of freedom, we end up with 16 (1,1) states, six (0,2) states and six (2,0) states; see appendix A.

2.1. Exchange interaction

The two quantum dots are coupled by the spin- and valley-preserving hopping (tunneling),

$$H_T = t \sum_{s\tau} \left(\hat{c}^{\dagger}_{2,s\tau} \hat{c}_{1,s\tau} + \text{h.c.} \right), \tag{4}$$

where t denotes the tunneling matrix element. We first consider the case without a magnetic field, $H_B = 0$, and the parameters in the regime $|t| \ll |U \pm \varepsilon|$ where the (1,1) charge states are approximate eigenstates of the Hamiltonian (1). The Pauli principle implies that only those (1,1) states are coupled to (0,2) and (2,0) states which are antisymmetric in the combined spin and valley space. In spin space, there is one antisymmetric state for two electrons, the spin singlet, and there are three symmetric states, the spin triplet states; for the valley space alone, the situation is analogous. To study the symmetric and antisymmetric states in the combined spin and valley space, we introduce vectors of Pauli matrices for the spin and valley of the electron in the first ($j = 1$) or second ($j = 2$) quantum dot, as $\mathbf{s}_j = (s_{jx}, s_{jy}, s_{jz})^{\mathrm{T}}$ and $\boldsymbol{\tau}_j = (\tau_{jx}, \tau_{jy}, \tau_{jz})^{\mathrm{T}}$, and express the projection on the singlet (upper index S) and the triplet (upper index T) sectors as follows:

$$P^{\mathrm{S}}_{\mathrm{spin}} = \frac{1 - \mathbf{s}_1 \cdot \mathbf{s}_2}{4}, \quad P^{\mathrm{T}}_{\mathrm{spin}} = \frac{\mathbf{s}_1 \cdot \mathbf{s}_2 + 3}{4}, \tag{5}$$

$$P^{\mathrm{S}}_{\mathrm{valley}} = \frac{1 - \boldsymbol{\tau}_1 \cdot \boldsymbol{\tau}_2}{4}, \quad P^{\mathrm{T}}_{\mathrm{valley}} = \frac{\boldsymbol{\tau}_1 \cdot \boldsymbol{\tau}_2 + 3}{4}. \tag{6}$$

These operators fulfill the usual relation for projectors, $\left(P^q_F\right)^2 = P^q_F$ and $P^{\mathrm{S}}_F + P^{\mathrm{T}}_F = 1$, where $F = \text{spin, valley}$ and $q = S, T$. The projection operator on the antisymmetric states of the combined spin and valley space is given by $P_{\mathrm{as}} = P^{\mathrm{S}}_{\mathrm{spin}} P^{\mathrm{T}}_{\mathrm{valley}} + P^{\mathrm{T}}_{\mathrm{spin}} P^{\mathrm{S}}_{\mathrm{valley}}$ and defines the effective low-energy Hamiltonian for the (1,1) states,

$$H_{\mathrm{eff}} = -J P_{\mathrm{as}} = \frac{J}{8}((\mathbf{s}_1 \cdot \mathbf{s}_2)(\boldsymbol{\tau}_1 \cdot \boldsymbol{\tau}_2) + \mathbf{s}_1 \cdot \mathbf{s}_2 + \boldsymbol{\tau}_1 \cdot \boldsymbol{\tau}_2 - 3). \tag{7}$$

The exchange coupling J is given by $J = 4t^2U/(U^2 - \varepsilon^2)$, which can be determined by a Schrieffer–Wolff transformation on H in the same way as it is used in the spin-only case [37]; see appendix B. The eigenvalues of H_{eff} are $-J$ and 0 with a six and a ten-dimensional eigenspace, respectively (see also [15]). The projection on the subspace with eigenenergy $-J$ is given in terms of spin and valley operators, but for the exchange coupling the origin of the degeneracy is irrelevant. Hence, the result we obtained here holds true for any fourfold degeneracy of the electron, provided that tunneling conserves this four-valued internal quantum number [38].

We can consider the reduced Hilbert space of the (1,1) states belonging to H_{eff} as a four-qubit space with the spins in the first and the second quantum dot as the first and the second

qubit and the valley iso-spins as qubits 3 and 4, with $|\uparrow\rangle \equiv |0\rangle$, $|\downarrow\rangle \equiv |1\rangle$, $|+\rangle \equiv |0\rangle$, $|-\rangle \equiv |1\rangle$. Using the four Bell states,

$$|\phi_\pm\rangle = \frac{|00\rangle \pm |11\rangle}{\sqrt{2}}, \quad |\psi_\pm\rangle = \frac{|01\rangle \pm |10\rangle}{\sqrt{2}}, \tag{8}$$

as basis states in the spin and valley space, and building a product basis,

$$\{|\phi_+\rangle, |\phi_-\rangle, |\psi_+\rangle, |\psi_-\rangle\}_{\text{spin}} \otimes \{|\phi_+\rangle, |\phi_-\rangle, |\psi_+\rangle, |\psi_-\rangle\}_{\text{valley}}, \tag{9}$$

the corresponding matrix of H_{eff} becomes diagonal. Obviously, we can identify $|\psi_-\rangle$ with the singlet and the other three vectors with the triplet space of the spin or the valley. We call (9) the *double Bell basis*.

2.2. Magnetic field

The influence of a magnetic field on the spin and the valley is given by

$$H_B = \sum_{j=1,2} h_{Sj}(\hat{n}_{j\uparrow} - \hat{n}_{j\downarrow}) + \sum_{j=1,2} h_{Vj}(\hat{n}_{j+} - \hat{n}_{j-}), \tag{10}$$

where the number operators are defined as $\hat{n}_{js} = \sum_\tau \hat{c}^\dagger_{js\tau}\hat{c}_{js\tau}$ and $\hat{n}_{j\tau} = \sum_s \hat{c}^\dagger_{js\tau}\hat{c}_{js\tau}$. The parameter h_{Sj} denotes the spin Zeeman energy in the jth quantum dot, where the spin quantization axis is chosen along the direction of the magnetic field. The valley degeneracy in each dot is broken by the magnetic-field component parallel to the axis of a CNT or orthogonal to the graphene sheet. This splitting is expressed as h_{Vj}, which we refer to as the valley Zeeman energy. It has been shown experimentally for a CNT [39] and theoretically for graphene quantum dots [32] that the valley Zeeman splitting due to this component of the magnetic field is much larger than the corresponding spin Zeeman splitting. On the other hand, the in-plane components in graphene and the components orthogonal to the axis of a CNT mainly influence the spin Zeeman energy. Therefore, the values of h_{Sj} and h_{Vj} can be set nearly independently by an external magnetic field.

We neglect here that the magnetic fields in the dots can have different directions, which would lead to additional avoided crossings in the spectrum of H. Under this condition, we can still apply the Schrieffer–Wolff transformation used in [37] to obtain an effective Hamiltonian for the 16 (1,1) states; see appendix B. We define $h_V = (h_{V1} + h_{V2})/2$, $h_S = (h_{S1} + h_{S2})/2$, $\Delta h_V = h_{V1} - h_{V2}$, and $\Delta h_S = h_{S1} - h_{S2}$. In the limit $|t|, |\Delta h_V|, |\Delta h_S| \ll |U \pm \varepsilon|$, we find that

$$H_{\text{eff},B} = \frac{J}{8}((\mathbf{s}_1 \cdot \mathbf{s}_2)(\boldsymbol{\tau}_1 \cdot \boldsymbol{\tau}_2) + \mathbf{s}_1 \cdot \mathbf{s}_2 + \boldsymbol{\tau}_1 \cdot \boldsymbol{\tau}_2 - 3) + \sum_{j=1,2}(h_{Sj}s_{jz} + h_{Vj}\tau_{jz})$$
$$+ \frac{J\varepsilon}{U^2 - \varepsilon^2}\left[\frac{\boldsymbol{\tau}_1 \cdot \boldsymbol{\tau}_2 - 1}{4}(s_{1z} + s_{2z})\Delta h_S + \frac{\mathbf{s}_1 \cdot \mathbf{s}_2 - 1}{4}(\tau_{1z} + \tau_{2z})\Delta h_V\right]. \tag{11}$$

The magnetic field might be a resource for tuning the exchange interaction, particularly in situations where the gradient is large and the linear approximation given here is not valid (for a more general expression, see appendix B). Nevertheless, we consider quantum gates created by the exchange coupling without a magnetic field in the following. More precisely, we assume that Δh_S and Δh_V are negligible while the exchange coupling is applied. This can be achieved if J as a function of time is tuned by varying ε. The parts of the Hamiltonian $H_{\text{eff},B}$ that depend on h_S and h_V commute with H_{eff} and can therefore be regarded as single-qubit operations performed before or after the exchange coupling is applied.

3. Controlled-NOT gate on spin qubits

In this section, we show that it is possible to perform a CNOT gate on the spin qubits alone,

$$\mathrm{CNOT}_{\mathrm{spin}} = \mathrm{CNOT} \otimes \mathbb{1} = \begin{pmatrix} 1 & 0 & 0 & 0 \\ 0 & 1 & 0 & 0 \\ 0 & 0 & 0 & 1 \\ 0 & 0 & 1 & 0 \end{pmatrix} \otimes \begin{pmatrix} 1 & 0 & 0 & 0 \\ 0 & 1 & 0 & 0 \\ 0 & 0 & 1 & 0 \\ 0 & 0 & 0 & 1 \end{pmatrix}, \tag{12}$$

by applying the exchange interaction (7), supplemented with single-qubit operations on both the spin and valley qubits. Note that in equation (12), the matrices are represented in the product basis of the qubit states (not in the Bell basis). Because CNOT gates can be combined with single-qubit gates to form arbitrary unitaries on any number of qubits [40, 41], our result below implies that universal quantum computing in the subspace of the spin qubits can be realized with the exchange interaction and single-qubit gates, despite the presence of valley degeneracy. For an explicit construction of a CNOT gate, we define the time-evolution operator $U(\phi)$ of the exchange interaction as

$$U(\phi) = \mathrm{e}^{-\mathrm{i}\int_0^{t_e} \mathrm{d}t'\, H_{\mathrm{eff}}(t')} = \mathbb{1} + \left(\mathrm{e}^{\mathrm{i}\phi} - 1\right) P_{\mathrm{as}}, \tag{13}$$

where $\phi = \int_0^{t_e} \mathrm{d}t'\, J(t')$ is the time-integrated exchange coupling and H_{eff} is the exchange Hamiltonian defined in equation (7). In the absence of valley degeneracy, e.g. $\tau_1 = \tau_2 = K$ and thus $\boldsymbol{\tau}_1 \cdot \boldsymbol{\tau}_2 = 1$ in equation (7), the exchange interaction directly generates a $\sqrt{\mathrm{SWAP}}$ gate for $\phi = \pi/2$,

$$\sqrt{\mathrm{SWAP}} = \frac{1+i}{2}\mathbb{1} + \frac{1-i}{2}\mathrm{SWAP}, \tag{14}$$

for the spin qubits, which can be applied twice in combination with single-spin rotations to generate CNOT [1]. Here, the SWAP gate simply exchanges the states of the two spin qubits. While the SWAP gate itself can also be obtained from the exchange interaction, it is not sufficient for constructing CNOT.

In the presence of valley degeneracy, a gate that interchanges the spin and valley qubits independently can be obtained similarly as in [1], as $U(\pm\pi) = \mathrm{SWAP} \otimes \mathrm{SWAP}$, or explicitly, $U(\pm\pi)|s_1, s_2, \tau_1, \tau_2\rangle = |s_2, s_1, \tau_2, \tau_1\rangle$. However, $U(\pm\pi/2) \neq \sqrt{\mathrm{SWAP}} \otimes \sqrt{\mathrm{SWAP}}$; instead, we find that

$$U(\pm\pi/2) = \frac{1 \pm i}{2}\mathbb{1} + \frac{1 \mp i}{2}\mathrm{SWAP} \otimes \mathrm{SWAP}. \tag{15}$$

In addition to producing the required entanglement between the two spins (and between the two valley iso-spins), this gate simultaneously also produces entanglement between the spin and the valley. To perform CNOT on the spin (or valley) alone, we thus need a modified pulse sequence. We find the following solution,

$$\sqrt{\mathrm{SWAP}}_{\mathrm{spin}} = \sqrt{\mathrm{SWAP}} \otimes \mathbb{1} = \mathrm{e}^{\mathrm{i}\frac{3\pi}{4}} \left(U(\pi/4)\tau_{1x} U(\pi/4)\tau_{1z}\right)^2, \tag{16}$$

from which we can construct a spin-only CNOT, using the result of [1],

$$\mathrm{CNOT}_{\mathrm{spin}} = \mathrm{i}\,\mathrm{e}^{-\mathrm{i}\frac{\pi}{4}s_{2y}}\, \mathrm{e}^{\mathrm{i}\frac{\pi}{4}(s_{2z}-s_{1z})} \sqrt{\mathrm{SWAP}}_{\mathrm{spin}}\, \mathrm{e}^{-\mathrm{i}\frac{\pi}{2}s_{1z}} \sqrt{\mathrm{SWAP}}_{\mathrm{spin}}\, \mathrm{e}^{\mathrm{i}\frac{\pi}{4}s_{2y}}, \tag{17}$$

where the signs of the spin rotations about the z-axis are opposite if one uses another root of SWAP, given as $\sqrt{\mathrm{SWAP}}^{-1}_{\mathrm{spin}}$, as in [1]. Note that $\sqrt{\mathrm{SWAP}}^{-1}_{\mathrm{spin}} = \sqrt{\mathrm{SWAP}}^{*}_{\mathrm{spin}}$ can be implemented

(up to a phase) by replacing $\pi/4$ by $-\pi/4$ in equation (16). The spin y-rotations in equation (17) implement a basis change that transforms CPHASE into the equivalent CNOT. The single-qubit gates τ_{1x} and τ_{1z} in equation (16) on the first valley qubit are implemented as $\exp(\mathrm{i}\frac{\pi}{2}\tau_{1\beta}) = \mathrm{i}\tau_{1\beta}$, where $\beta = x, y, z$. Another possibility to write the sequence for $\sqrt{\mathrm{SWAP}}_{\mathrm{spin}}$ is

$$\sqrt{\mathrm{SWAP}}_{\mathrm{spin}} = \mathrm{e}^{-\mathrm{i}\frac{\pi}{4}} U(\pi/4) \prod_{\beta=x,y,z} \tau_{1\beta} U(\pi/4) \tau_{1\beta}, \tag{18}$$

which reflects the symmetry of the gate under permutation of the Pauli matrices τ_{1x}, τ_{1y} and τ_{1z}. Note that equation (18) can easily be checked because $U(\phi)$, $\tau_{1\beta}U(\pi/4)\tau_{1\beta}$ ($\beta = x, y, z$) and $\sqrt{\mathrm{SWAP}}_{\mathrm{spin}}$ are diagonal in the double Bell basis (9). Equation (17) describes a CNOT gate for the spin qubits that does not affect the valley states. The fact that a CNOT gate exclusively on the spin qubits can be performed as in equation (17) by using the new sequence equation (16) in a valley-degenerate system is the first main result of this paper. By simply exchanging the single-qubit spin and valley operators ($s \leftrightarrow \tau$) in the equations above, we also find a CNOT gate in valley space which does not affect the spins. Here, we have assumed that arbitrary single-qubit operations in spin and valley space are available. The implementation of valley rotations within nanosecond time scales using electron valley resonance in a CNT has been proposed in [42]. Finally, we note that while full valley coherence is needed when the valley states are used as qubits (see section 5), this is not required for the 'valley-assisted' spin-qubit gate $\sqrt{\mathrm{SWAP}}_{\mathrm{spin}}$, equation (16), and thus for CNOT, because the spin and valley operations ultimately factorize. Even if the initial valley state is mixed, the valley iso-spin will be disentangled by the end of the gate operation, leaving the spin qubit sector coherent. However, there is a somewhat less stringent restriction on valley coherence: any valley qubit error (bit or phase flip) which occurs *during* the gate operation can propagate into the spin sector. While we do not have sufficient experimental data on valley coherence to determine whether this condition will be fulfilled, we note that at least this condition is much easier to satisfy than full valley coherence. Starting from the estimated Rabi period for electron valley resonance [42], we expect the relevant gate operation time to be around 10 ns.

4. State preparation and measurement

Before we describe how state preparation and projective measurements can be carried out in a valley-degenerate system, we briefly characterize the situation in the spin-only case, which has already been explored experimentally [2, 5, 6]. In a double quantum dot without a valley degree of freedom, the Pauli principle allows only one state with a (0,2) charge distribution. In the case $\varepsilon \gg U$, this is the ground state of the system. Therefore, state preparation is possible by waiting at a large value of ε until the double quantum dot relaxes to this ground state. Afterwards, ε can be reduced to zero adiabatically which drives the system to one specific (1,1) charge state, selected by the magnetic field (for $B = 0$, the spin singlet). Reading out a qubit state can be achieved by increasing ε adiabatically, thus allowing a projective measurement on the one specific (1,1) state that is connected to the (0,2) state, while all other states remain in a (1,1) charge distribution. The charge distribution can then be measured with a charge sensor, e.g. a quantum point contact.

In the presence of the valley degree of freedom, the situation is more complicated because there are six linearly independent (0,2) states. In order to prepare the system in a well-known initial state by a relaxation process, this sixfold degeneracy has to be lifted. This can be done

Table 1. Charge detection in the presence of valley degeneracy. For each of the eight different configurations of Δh_S and Δh_V, the letter x in the table indicates the six basis states that make a transition to a (0,2) state if ε is adiabatically changed from 0 to $\varepsilon > U$. The gray columns belong to the configurations of the magnetic field that are used in the example in the text.

	$\Delta h_S > \Delta h_V > 0$	$\Delta h_V > \Delta h_S > 0$	$\Delta h_S > 0 > \Delta h_V, \Delta h_S > \lvert\Delta h_V\rvert$	$\Delta h_S > 0 > \Delta h_V, \Delta h_S < \lvert\Delta h_V\rvert$	$\Delta h_V > 0 > \Delta h_S, \Delta h_V > \lvert\Delta h_S\rvert$	$\Delta h_V > 0 > \Delta h_S, \Delta h_V < \lvert\Delta h_S\rvert$	$0 > \Delta h_V > \Delta h_S$	$0 > \Delta h_S > \Delta h_V$
$\lvert\uparrow,\uparrow,+,+\rangle$								
$\lvert\uparrow,\uparrow,+,-\rangle$			x	x			x	x
$\lvert\uparrow,\uparrow,-,+\rangle$	x	x			x	x		
$\lvert\uparrow,\uparrow,-,-\rangle$								
$\lvert\uparrow,\downarrow,+,+\rangle$					x	x	x	x
$\lvert\uparrow,\downarrow,+,-\rangle$				x		x	x	x
$\lvert\uparrow,\downarrow,-,+\rangle$		x			x	x	x	
$\lvert\uparrow,\downarrow,-,-\rangle$					x	x	x	x
$\lvert\downarrow,\uparrow,+,+\rangle$	x	x	x	x				
$\lvert\downarrow,\uparrow,+,-\rangle$	x		x	x				x
$\lvert\downarrow,\uparrow,-,+\rangle$	x	x	x		x			
$\lvert\downarrow,\uparrow,-,-\rangle$	x	x	x	x				
$\lvert\downarrow,\downarrow,+,+\rangle$								
$\lvert\downarrow,\downarrow,+,-\rangle$			x	x			x	x
$\lvert\downarrow,\downarrow,-,+\rangle$	x	x			x	x		
$\lvert\downarrow,\downarrow,-,-\rangle$								

using the spin or valley Zeeman term, i.e. by applying a magnetic field. Measuring the charge state after increasing the value of ε realizes a projection on a six- or a ten-dimensional subspace, when the system goes over to a (0,2) charge state or stays in a (1,1) state, respectively. To achieve a projective measurement on a single quantum state, several charge measurements can be carried out in series. By applying a proper external magnetic field it is possible to influence which states are connected to a (0,2) state by the adiabatic transition described above. Assuming that for $\varepsilon = 0$ the exchange interaction $J = 4t^2/U$ is small compared to h_F and Δh_F with $F = S, V$, the states $|s_1, s_2, \tau_1, \tau_2\rangle$ with $s_j = \uparrow, \downarrow$ and $\tau_j = \pm$ are approximate eigenstates of the Hamiltonian (1). Figure 2 shows the eigenenergies as a function of ε for the situation $\Delta h_S > \Delta h_V > 0$. The six states that are converted into (0,2) states by increasing ε show a nearly linear dependence on ε for $\varepsilon > U$. Which states develop into a (0,2) state depends on the signs of Δh_S, Δh_V and $|\Delta h_S| - |\Delta h_V|$, giving rise to $2^3 = 8$ different configurations to be distinguished (table 1). In the following, we explicitly describe two procedures for implementing a projective measurement onto one specific state.

For the first procedure, we additionally presume that the magnetic field can be changed in order to reach different configurations for the charge measurement as given in table 1. This means that after the first charge measurement at $\varepsilon > U$, which projects the state onto a six- or a ten-dimensional subspace, and subsequently reducing ε to zero, it is possible to change the magnetic field, perform a new adiabatic transition and make a new measurement of the charge

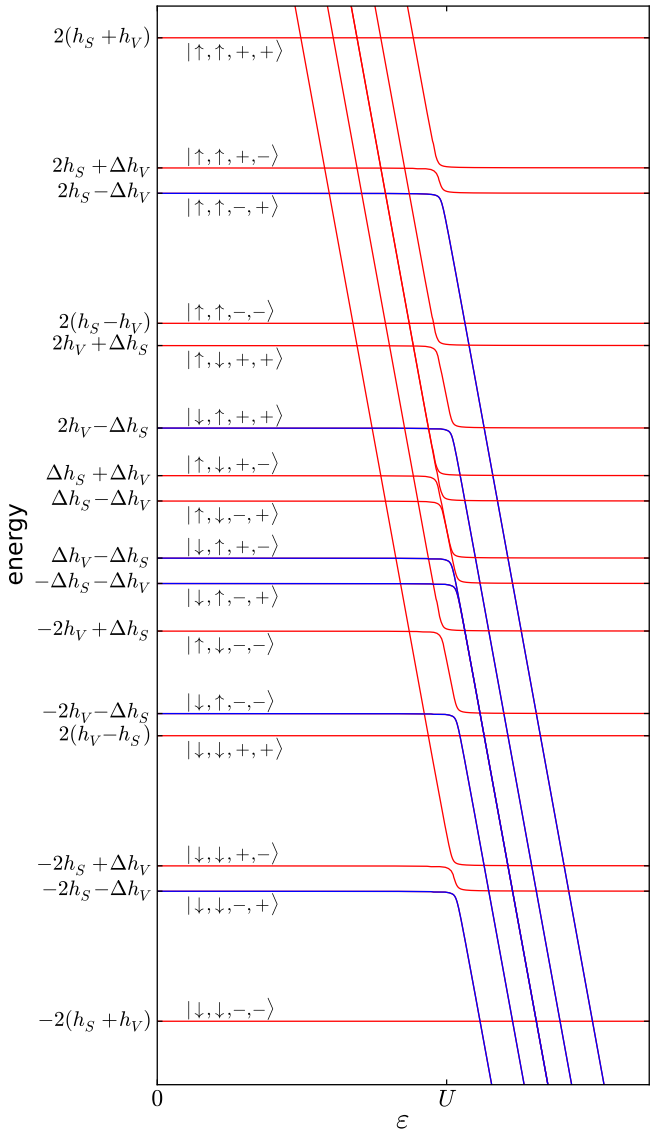

Figure 2. Double-dot two-electron energy spectrum described by equation (1) as a function of the asymmetry ε. Here, the magnetic field fulfills $\Delta h_S > \Delta h_V > 0$ and the exchange energy at $\varepsilon = 0$ is small compared to h_F and Δh_F with $F = S, V$. The six darker (blue) lines indicate which states are connected to the (0,2) space by an adiabatic transition, while the brighter (red) lines denote states that remain in the (1,1) space even at large asymmetries. Note that the central dark (blue) line is twofold degenerate in the limit of large ε.

distribution. We now consider the example of three charge measurements with the following three different configurations of the magnetic field: (i) $\Delta h_S > \Delta h_V > 0$; (ii) $\Delta h_S > 0 > \Delta h_V$, $\Delta h_S > |\Delta h_V|$; (iii) $\Delta h_V > 0 > \Delta h_S$, $\Delta h_V > |\Delta h_S|$. By considering these three cases in table 1, one finds that only the state $|\downarrow,\uparrow,-,+\rangle$ belongs in all three cases to the six-dimensional subspace corresponding to a measurement of a (0,2) charge state. Therefore, the three charge measurements with outcome (0,2) amount to a projection on the state.

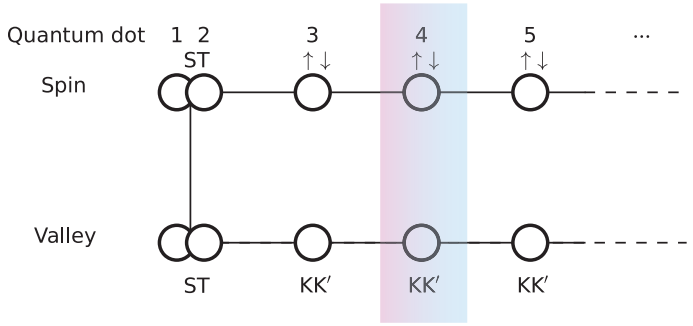

Figure 3. Quantum register using both spin and valley qubits. The shaded area indicates one quantum dot (number 4) occupied by one electron. Each quantum dot is represented by two circles, one for the spin and one for the valley isospin. The electrons in quantum dots 1 and 2 act as singlet–triplet (ST) qubits to allow for universal two-qubit gates between the spin and the valley. In all other quantum dots, we consider usual single-electron spin and valley qubits, $\uparrow\downarrow$ and KK', respectively.

For the second procedure, we use a time-independent magnetic field, for example in the configuration $\Delta h_S > \Delta h_V > 0$. Instead of changing the magnetic field, we change the state by single-qubit operations applied when $\varepsilon = 0$. In our example we may apply $e^{i\pi s_{1x}/2}$, flipping the first spin, after the first charge measurement and $e^{i\pi s_{2x}/2}$, flipping the second spin, after the second charge measurement. The state $|\uparrow,\uparrow,-,+\rangle$ is the only state that is mapped after the first and the second spin flip to the six-dimensional subspace which corresponds to (0,2) states after the adiabatic transition, thus measuring three times a (0,2) charge configuration is again a projection on one specific state. If single-qubit operations for all qubits are feasible, any $|s_1, s_2, \tau_1, \tau_2\rangle$ can be mapped to $|\downarrow,\uparrow,-,+\rangle$ or $|\uparrow,\uparrow,-,+\rangle$. Therefore, projection on any of these 16 states can be done in this way.

5. Quantum register combining spin and valley qubits

So far, we have shown that universal two-qubit gates between spin qubits or between valley qubits can be implemented. We now consider the situation when both the valley and the spin serve as qubits. Note that using valley qubits in a quantum register requires valley coherence times that are sufficiently long to allow for quantum error correction. This is a stricter requirement than in the situation when valley operations are only needed to achieve spin manipulation (see section 3). If both types of qubits are to be combined in the same quantum register it is necessary to find a two-qubit gate between a spin and a valley qubit. Here we show that this can be done using singlet–triplet qubits in the spin and valley space in one double quantum dot. For these singlet–triplet qubits the exchange interaction leads directly to a universal two-qubit gate, as explained in section 5.1. Then, in section 5.2, we show how to connect these qubits to the usual single-electron spin and valley qubits. This leads effectively to a chain of qubits where nearest neighbors are connected by universal two-qubit gates, as shown in figure 3. If N is the number of quantum dots, the number of qubits in this register is given by $2(N-1)$.

5.1. Singlet–triplet qubits

In this subsection, we briefly investigate a different qubit implementation, in which the singlet state $|\psi_-\rangle \equiv |0\rangle$ and the triplet state $|\psi_+\rangle \equiv |1\rangle$ (see equation (8)) in the spin and valley space are used as the qubit basis states. Hence, we consider only a subspace of all (1,1) charge states as the logic space. Since only one out of three triplet states is part of this logic space, the effective Hamiltonian in the basis $\{|\psi_-\rangle, |\psi_+\rangle\}_{\text{spin}} \otimes \{|\psi_-\rangle, |\psi_+\rangle\}_{\text{valley}}$ assumes the simple diagonal form $H_{\text{eff}} = \text{diag}(0, -J, -J, 0)$. Using the Makhlin invariants [43], it is now easy to show that the unitary evolution $U(\pi/2) = \text{diag}(1, i, i, 1)$ generated by this Hamiltonian is equivalent to a CNOT gate, i.e. it equals CNOT up to single-qubit operations. Therefore, in this subspace we are able to connect a spin and a valley qubit with a universal two-qubit gate by applying the exchange interaction. We define $\sigma_\beta^{(k)}$ $(\beta = x, y, z)$ as the Pauli matrices in the singlet–triplet basis for the spin $(k = 1)$ and the valley $(k = 2)$. Single-qubit operations can then be performed as follows. A magnetic field gradient between the dots acts in the singlet–triplet basis as a single-qubit rotation $\sigma_x^{(k)}$ as any difference in Zeeman splitting between the first and the second spin or valley corresponds to a rotation in the singlet–triplet basis. The gates $\sigma_z^{(k)}$ can be realized by applying the exchange interaction and valley or spin rotations as $\exp(\mathrm{i}\theta\sigma_z^{(1)}) = \mathrm{e}^{\mathrm{i}\theta}\tau_{1x}U(-2\theta)\tau_{1x}$ and analogously for $\sigma_z^{(2)}$ by replacing τ_{1x} with s_{1x}. These single-qubit gates, together with the universal two-qubit gate, allow universal quantum computing in this two-qubit space.

5.2. Two-qubit gate between a single-electron and a singlet–triplet qubit

In section 3, we have shown that any two-qubit gate can be applied between two neighboring spin or valley qubits. We now consider three quantum dots where the spin and the valley in dots 1 and 2 are prepared in states that are linear combinations of $|\psi_+\rangle$ and $|\psi_-\rangle$, whereas the spin and the valley of the third dot can be in any possible state (figure 3). To couple the single-spin qubit in dot 3 to the singlet–triplet spin qubit in dots 1 and 2, we apply a CPHASE gate between the spins of the electrons in the third and the second dot where the spin of the third dot is the control qubit. The spin state of the first and the second quantum dot remains in the subspace $\{|\psi_+\rangle, |\psi_-\rangle\}$ after this operation. As s_{2z} represents a change in the relative phase between spins 1 and 2, thus exchanging singlet and triplet states, it acts as a $\sigma_x^{(1)}$ gate in the singlet–triplet basis; thus this CPHASE gate between the spins is a CNOT gate in terms of the qubits if they are defined as a usual spin-up/spin-down qubit in the third quantum dot and a singlet–triplet qubit in the first two dots. A CNOT gate for the valley can be implemented analogously. Consequently, any two-qubit gate between a usual single-electron and a singlet–triplet qubit can be applied.

6. Conclusions and outlook

In this paper, we have shown that in the presence of valley degeneracy, a CNOT gate on spin qubits in a double quantum dot can be constructed from a sequence of single-qubit operations and the exchange interaction. A CNOT gate on the valley qubits can be generated analogously. For initialization and measurement, an inhomogeneous external magnetic field is necessary. A projection on one specific state can be constructed from three charge measurements either under different configurations of the magnetic field or by using single-qubit gates. We could show that adding one double quantum dot in the singlet–triplet mode allows for a universal quantum gate (e.g. CNOT) between a spin and a valley qubit. This connection between the spin and the valley qubits in a quantum register implies that universal quantum computing based on

spin and valley qubits stored in the same quantum dots is possible in principle. Nevertheless, the realization of coherent manipulation of spin and valley qubits in carbon materials is certainly a big challenge. An important precondition would be that the valley degree of freedom has a sufficiently long coherence time, which is currently unknown. An alternative way to create a spin–valley quantum register may lie in extending the singlet–triplet architecture with spin and valley degrees of freedom beyond two qubits, e.g. along the lines of [44, 45] for spin-only qubits.

Every quantum computing approach can only be realized for sufficiently long coherence times T_2 and relaxation times T_1 allowing coherent quantum gates (the latter also allowing for high-fidelity projective measurements). At low temperatures, the electron spin relaxation time was measured to be of the order of hours [46], the decoherence time has recently be shown to reach 10 s [47] for isotopically enriched ^{28}Si limited in this experiment by donor impurities [48]. Coherent spin manipulation experiments in Si/SiGe quantum dots [20] could already be performed showing an improvement of the dephasing time compared to GaAs. For CNT and graphene quantum dots, theory predicts coherence times of the order of 100 μs for the natural abundance of ^{13}C [49]. For the quantum gate schemes presented in this paper, also the relaxation and coherence times of the valley states have to be sufficiently long (how long depends on the specific scheme to be implemented). While the valley coherence and relaxation times in nanotubes and graphene are to a large extent unknown, the potential sources of decoherence are presumably the hyperfine interaction [50], atomic disorder [42], and in the case of a dependence on an external magnetic or electric field, also the fluctuations of those fields. A recent experiment [51] reports a lower bound of 48 ns for the valley relaxation time in Si from a transport measurement. Possible valley relaxation processes include impurity scattering and electron–phonon interaction. Note that the exchange interaction as the origin of two-qubit gates in this paper works by the same mechanism as in the spin-only case. For the decoherence due to charge fluctuations during the time that the singlet state is a mixture of (1,1) and (0,2) charge states, the same consideration as in the spin-only case can be applied [52].

In this work, we have neglected the influence of spin–orbit interaction, although it can have important effects on CNT quantum dots [39, 53]. It will be a very interesting task to develop a theory for quantum computing with full orbital and spin degrees of freedom in a regime dominated by spin–orbit coupling. Despite the proof-of-principle results provided here, there are, obviously, some remaining open problems regarding the construction of quantum gates with the exchange interaction with two degrees of freedom (spin and valley). It is at present not clear whether there is a shorter sequence for the $\sqrt{\text{SWAP}}$ gate on spin qubits than equation (16). Also, we did not find a *direct* CNOT (or SWAP) gate, i.e. without the use of singlet–triplet qubits, applied between one single-electron spin and one single-electron valley qubit, although the exchange interaction also couples spins and valleys. Further efforts could go into finding a simpler or even optimal gate implementation for a spin–valley qubit register. The time-evolution operators acting on a four-qubit Hilbert space are, if we fix the irrelevant global phase, elements of the special unitary group $SU(16)$, which is a $16^2 - 1 = 255$-dimensional space, whereas a unitary operation on a two-qubit space lies in $SU(4)$, which has only 15 dimensions, and its two-qubit part can even be described by three real parameters [43, 54]. The sequence for the $\sqrt{\text{SWAP}}_{\text{spin}}$ gate given in equation (16) follows from equation (18), which is relatively easy to find as it is constructed as a product of unitary operations that are diagonal in the double Bell basis. We now face the more general task of finding a desired quantum gate for a given sequence of exchange interactions and single-qubit gates where the pulse lengths (gate times) are free parameters to be determined. This can be attempted numerically by minimizing a scalar function

that quantifies the difference between the desired gate and the gate obtained for a given set of parameters [55]. If the desired gate is an element of $SU(4) \otimes SU(4) \subset SU(16)$, e.g. a two-qubit gate between one spin and one valley iso-spin, we can quantify the deviation from this subspace and use the Makhlin invariants to describe only the two-qubit part in both $SU(4)$ factors. This reduces the dimension to 231. Nonetheless, the search for quantum gates constructed with a four-qubit interaction and single-qubit operations remains a challenging problem.

Acknowledgments

The authors acknowledge financial support from DFG under the programs SPP 1285 'Semiconductor spintronics' and SFB 767 'Functional nanostructures'.

Appendix A. Two-electron states in spin- and valley-degenerate double dots

In a quantum dot with spin and twofold valley degrees of freedom there are four possible states if we restrict ourselves to the lowest orbital in the dot. If we consider two electrons in two dots, i.e. two fermions in eight one-particle states, then we obtain a system with $\binom{8}{2} = 28$ states, where the charge configurations (1,1), (2,0) and (0,2) are possible. Note that any fermionic state has to be antisymmetric; thus it is convenient to use the Bell states for spin and valley as introduced in equation (8) as this basis distinguishes between antisymmetric ($|\psi_-\rangle$) and symmetric states ($|\psi_+\rangle$, $|\phi_+\rangle$, $|\phi_-\rangle$). In the (1,1) charge configuration the spatial wavefunction can be either symmetric or antisymmetric and therefore any product of a Bell state in the spin and a Bell state in the valley degree of freedom is permitted, which leads to 16 (1,1) states. As for (2,0) or (0,2) charge configuration, the spatial wavefunction can only be symmetric, the product of spin and valley states has to be antisymmetric, i.e. it has to be either a product of the antisymmetric spin singlet $|\psi_-\rangle_{\text{spin}}$ and a symmetric valley state ($|\psi_+\rangle_{\text{valley}}$, $|\phi_\pm\rangle_{\text{valley}}$) or vice versa. This amounts to six (2,0) and six (0,2) states corresponding to two fermions in four one-particle states, $\binom{4}{2} = 6$. Here we provide all 28 basis states denoted by the charge configuration and as products of Bell states for the spin and the valley degree of freedom:

$$
\begin{array}{lll}
(1,1)|\psi_-\rangle_{\text{spin}}|\psi_+\rangle_{\text{valley}} & (2,0)|\psi_-\rangle_{\text{spin}}|\psi_+\rangle_{\text{valley}} & (0,2)|\psi_-\rangle_{\text{spin}}|\psi_+\rangle_{\text{valley}} \\
(1,1)|\psi_-\rangle_{\text{spin}}|\phi_+\rangle_{\text{valley}} & (2,0)|\psi_-\rangle_{\text{spin}}|\phi_+\rangle_{\text{valley}} & (0,2)|\psi_-\rangle_{\text{spin}}|\phi_+\rangle_{\text{valley}} \\
(1,1)|\psi_-\rangle_{\text{spin}}|\phi_-\rangle_{\text{valley}} & (2,0)|\psi_-\rangle_{\text{spin}}|\phi_-\rangle_{\text{valley}} & (0,2)|\psi_-\rangle_{\text{spin}}|\phi_-\rangle_{\text{valley}} \\
(1,1)|\psi_+\rangle_{\text{spin}}|\psi_-\rangle_{\text{valley}} & (2,0)|\psi_+\rangle_{\text{spin}}|\psi_-\rangle_{\text{valley}} & (0,2)|\psi_+\rangle_{\text{spin}}|\psi_-\rangle_{\text{valley}} \\
(1,1)|\phi_+\rangle_{\text{spin}}|\psi_-\rangle_{\text{valley}} & (2,0)|\phi_+\rangle_{\text{spin}}|\psi_-\rangle_{\text{valley}} & (0,2)|\phi_+\rangle_{\text{spin}}|\psi_-\rangle_{\text{valley}} \\
(1,1)|\phi_-\rangle_{\text{spin}}|\psi_-\rangle_{\text{valley}} & (2,0)|\phi_-\rangle_{\text{spin}}|\psi_-\rangle_{\text{valley}} & (0,2)|\phi_-\rangle_{\text{spin}}|\psi_-\rangle_{\text{valley}} \\
(1,1)|\psi_-\rangle_{\text{spin}}|\psi_-\rangle_{\text{valley}} & & \\
(1,1)|\psi_+\rangle_{\text{spin}}|\psi_+\rangle_{\text{valley}} & & \\
(1,1)|\psi_+\rangle_{\text{spin}}|\phi_+\rangle_{\text{valley}} & & \\
(1,1)|\psi_+\rangle_{\text{spin}}|\phi_-\rangle_{\text{valley}} & & \\
(1,1)|\phi_+\rangle_{\text{spin}}|\psi_+\rangle_{\text{valley}} & & \\
(1,1)|\phi_+\rangle_{\text{spin}}|\phi_+\rangle_{\text{valley}} & & \\
(1,1)|\phi_+\rangle_{\text{spin}}|\phi_-\rangle_{\text{valley}} & & \\
(1,1)|\phi_-\rangle_{\text{spin}}|\psi_+\rangle_{\text{valley}} & & \\
(1,1)|\phi_-\rangle_{\text{spin}}|\phi_+\rangle_{\text{valley}} & & \\
(1,1)|\phi_-\rangle_{\text{spin}}|\phi_-\rangle_{\text{valley}} & &
\end{array}
\tag{A.1}
$$

Appendix B. Effective Hamiltonian in the presence of a magnetic field

The Hamiltonian (1) in the presence of a magnetic field with the same direction in both dots (see section 2.2) can be written as a 28×28 matrix consisting of seven independent 4×4 submatrices, by using the following basis set:

$$\text{block } 1\{c^\dagger_{1,\uparrow+}c^\dagger_{2,\uparrow+}|0\rangle, c^\dagger_{1,\uparrow-}c^\dagger_{2,\uparrow-}|0\rangle, c^\dagger_{1,\downarrow+}c^\dagger_{2,\downarrow+}|0\rangle, c^\dagger_{1,\downarrow-}c^\dagger_{2,\downarrow-}|0\rangle\}, \tag{B.1}$$

$$\text{block } 2\{c^\dagger_{1,\uparrow+}c^\dagger_{2,\uparrow-}|0\rangle, c^\dagger_{1,\uparrow-}c^\dagger_{2,\uparrow+}|0\rangle, c^\dagger_{1,\uparrow+}c^\dagger_{1,\uparrow-}|0\rangle, c^\dagger_{2,\uparrow+}c^\dagger_{2,\uparrow-}|0\rangle\}, \tag{B.2}$$

$$\text{block } 3\{c^\dagger_{1,\downarrow+}c^\dagger_{2,\downarrow-}|0\rangle, c^\dagger_{1,\downarrow-}c^\dagger_{2,\downarrow+}|0\rangle, c^\dagger_{1,\downarrow+}c^\dagger_{1,\downarrow-}|0\rangle, c^\dagger_{2,\downarrow+}c^\dagger_{2,\downarrow-}|0\rangle\}, \tag{B.3}$$

$$\text{block } 4\{c^\dagger_{1,\uparrow+}c^\dagger_{2,\downarrow+}|0\rangle, c^\dagger_{1,\downarrow+}c^\dagger_{2,\uparrow+}|0\rangle, c^\dagger_{1,\uparrow+}c^\dagger_{1,\downarrow+}|0\rangle, c^\dagger_{2,\uparrow+}c^\dagger_{2,\downarrow+}|0\rangle\}, \tag{B.4}$$

$$\text{block } 5\{c^\dagger_{1,\uparrow-}c^\dagger_{2,\downarrow-}|0\rangle, c^\dagger_{1,\downarrow-}c^\dagger_{2,\uparrow-}|0\rangle, c^\dagger_{1,\uparrow-}c^\dagger_{1,\downarrow-}|0\rangle, c^\dagger_{2,\uparrow-}c^\dagger_{2,\downarrow-}|0\rangle\}, \tag{B.5}$$

$$\text{block } 6\{c^\dagger_{1,\uparrow+}c^\dagger_{2,\downarrow-}|0\rangle, c^\dagger_{1,\downarrow-}c^\dagger_{2,\uparrow+}|0\rangle, c^\dagger_{1,\uparrow+}c^\dagger_{1,\downarrow-}|0\rangle, c^\dagger_{2,\uparrow+}c^\dagger_{2,\downarrow-}|0\rangle\}, \tag{B.6}$$

$$\text{block } 7\{c^\dagger_{1,\downarrow+}c^\dagger_{2,\uparrow-}|0\rangle, c^\dagger_{1,\uparrow-}c^\dagger_{2,\downarrow+}|0\rangle, c^\dagger_{1,\downarrow+}c^\dagger_{1,\uparrow-}|0\rangle, c^\dagger_{2,\downarrow+}c^\dagger_{2,\uparrow-}|0\rangle\}. \tag{B.7}$$

We call the seven submatrices $H_1, \ldots, H_7$ and find that

$$H_1 = \mathrm{diag}(2(h_S + h_V), 2(h_S - h_V), 2(h_V - h_S), -2(h_S + h_V)), \tag{B.8}$$

which is not affected by the exchange interaction as block 1 only contains triplet states, and

$$H_j = C\mathbb{1}_4 + \begin{pmatrix} A & 0 & t & t \\ 0 & -A & -t & -t \\ t & -t & U+B & 0 \\ t & -t & 0 & U-B \end{pmatrix}, \tag{B.9}$$

with

$$\begin{aligned}
&j = 2 : A = \Delta h_V,\ B = \varepsilon + \Delta h_S,\ C = 2h_S;\\
&j = 3 : A = \Delta h_V,\ B = \varepsilon - \Delta h_S,\ C = -2h_S;\\
&j = 4 : A = \Delta h_S,\ B = \varepsilon + \Delta h_V,\ C = 2h_V;\\
&j = 5 : A = \Delta h_S,\ B = \varepsilon - \Delta h_V,\ C = -2h_V;\\
&j = 6 : A = \Delta h_V + \Delta h_S,\ B = \varepsilon,\ C = 0;\\
&j = 7 : A = \Delta h_V - \Delta h_S,\ B = \varepsilon,\ C = 0.
\end{aligned}$$

A simple unitary transformation,

$$W = \frac{1}{\sqrt{2}} \begin{pmatrix} 1 & 1 & 0 & 0 \\ 1 & -1 & 0 & 0 \\ 0 & 0 & 1 & 1 \\ 0 & 0 & 1 & -1 \end{pmatrix} \tag{B.10}$$

leads to the matrix form

$$W H_j W^\dagger = \begin{pmatrix} 0 & A & 0 & 0 \\ A & 0 & 2t & 0 \\ 0 & 2t & U & B \\ 0 & 0 & B & U \end{pmatrix} + C\mathbb{1}_4 \quad (j = 2, \ldots, 7), \tag{B.11}$$

where the 2×2 block in the upper left corner affects only (1,1), while those in the lower right corner affect only (2,0) and (0,2) charge states. These blocks are the part $H_0^{(j)} + H_B^{(j)}$ of the Hamiltonian (1) where $j = 2, \ldots, 7$. The rest of the Hamiltonian, $H_T^{(j)}$, which describes the hopping, couples the subspaces which are symmetric and asymmetric in charge. Hamiltonians written in such a matrix form occur already in the spin-only case and have been considered in [37], where a Schrieffer–Wolff transformation is used to derive an effective Hamiltonian for the sixteen (1,1) states. When we omit the index j for better readability, the Schrieffer–Wolff transformation can be written as $\tilde{H} = \mathrm{e}^{-S} W H W^{\dagger} \mathrm{e}^{S} \approx H_0 + H_B + [H_T, S]/2$ with $S = -S^{\dagger}$ and $[H_0 + H_B, S] = -H_T$. The approximation holds for $|t| \ll |U \pm B|$. We can use the result of [37] and find that $\tilde{H}$ is in lowest order given by two independent 2×2 matrices. The matrix describing the subspace with nearly (1,1) charge distribution has the form

$$\begin{pmatrix} 0 & \tilde{A} \\ \tilde{A} & -\tilde{J} \end{pmatrix} + C\mathbb{1}_2, \tag{B.12}$$

with

$$\tilde{J} = \frac{4t^2U(U^2 - B^2 - A^2)}{U^4 + B^4 + A^4 - 2U^2B^2 - 2U^2B^2 - 2B^2A^2} \tag{B.13}$$

and

$$\tilde{A} = A\left(1 - \frac{J(U^2 + B^2 - A^2)}{4U(U^2 - B^2 - A^2)}\right). \tag{B.14}$$

In the case of small gradients in the magnetic field and thus small differences in Zeeman splitting between the dots, we can expand these terms and find in lowest order of Δh_V and Δh_S (the index refers again to the blocks in the basis set)

$$\tilde{J}_{2/3} \approx \frac{4t^2U}{U^2 - \varepsilon^2} \pm \frac{8t^2U\varepsilon}{(U^2 - \varepsilon^2)^2}\Delta h_S = J\left(1 \pm \frac{2\varepsilon\Delta h_S}{U^2 - \varepsilon^2}\right), \tag{B.15}$$

$$\tilde{J}_{4/5} \approx \frac{4t^2U}{U^2 - \varepsilon^2} \pm \frac{8t^2U\varepsilon}{(U^2 - \varepsilon^2)^2}\Delta h_V = J\left(1 \pm \frac{2\varepsilon\Delta h_V}{U^2 - \varepsilon^2}\right), \tag{B.16}$$

$$\tilde{J}_{6/7} \approx \frac{4t^2U}{U^2 - \varepsilon^2} = J, \tag{B.17}$$

and $\tilde{A} \approx A$. Expressed with the Pauli matrices for the spin and the valley, this gives the effective Hamiltonian of equation (11) for the states which have approximately (1,1) charge distribution.

Note that we did not use the double Bell basis (see section 2.1) in this appendix as this does not provide the matrix form of the Hamiltonian with independent 4×4 submatrices in the presence of a magnetic field. Without a magnetic field the result for the splitting due to exchange interaction is $\tilde{J} = 4t^2U/(U^2 - \varepsilon^2) = J$ for all blocks $2, \ldots, 7$. In this case, the double Bell basis can be obtained by linear combinations of the basis vectors used here only within the degenerate six- and ten-dimensional subspaces. Therefore, the effective Hamiltonian is diagonal in the double Bell basis if no magnetic field is applied.

References

[1] Loss D and DiVincenzo D P 1998 Quantum computation with quantum dots *Phys. Rev.* A **57** 120

[2] Petta J R, Johnson A C, Taylor J M, Laird E A, Yacoby A, Lukin M D, Marcus C M, Hanson M P and Gossard A C 2005 Coherent manipulation of coupled electron spins in semiconductor quantum dots *Science* **309** 2180

[3] Koppens F H L, Buizert C, Tielrooij K J, Vink I T, Nowack K C, Meunier T, Kouwenhoven L P and Vandersypen L M K 2006 Driven coherent oscillations of a single electron spin in a quantum dot *Nature* **442** 766

[4] Foletti S, Bluhm H, Mahalu D, Umansky V and Yacoby A 2009 Universal quantum control of two-electron spin quantum bits using dynamic nuclear polarization. *Nature Phys.* **5** 903

[5] Brunner R, Shin Y-S, Obata T, Pioro-Ladrière M, Kubo T , Yoshida K, Taniyama T, Tokura Y and Tarucha S 2011 Two-qubit gate of combined single-spin rotation and interdot spin exchange in a double quantum dot *Phys. Rev. Lett.* **107** 146801

[6] Hanson R, Kouwenhoven L P, Petta J R, Tarucha S and Vandersypen L M K 2007 Spins in few-electron quantum dots *Rev. Mod. Phys.* **79** 1217–65

[7] Recher P and Trauzettel B 2010 Quantum dots and spin qubits in graphene *Nanotechnology* **21** 302001

[8] Trauzettel B, Bulaev D V, Loss D and Burkard G 2007 Spin qubits in graphene quantum dots *Nature Phys.* **3** 192

[9] Güttinger J, Frey T, Stampfer C, Ihn T and Ensslin K 2010 Spin states in graphene quantum dots *Phys. Rev. Lett.* **105** 116801

[10] Buitelaar M R, Bachtold A, Nussbaumer T, Iqbal M and Schönenberger C 2002 Multiwall carbon nanotubes as quantum dots *Phys. Rev. Lett.* **88** 156801

[11] Liang W, Bockrath M and Park H 2002 Shell filling and exchange coupling in metallic single-walled carbon nanotubes *Phys. Rev. Lett.* **88** 126801

[12] Cobden D H and Nygård J 2002 Shell filling in closed single-wall carbon nanotube quantum dots *Phys. Rev. Lett.* **89** 046803

[13] Churchill H O H, Kuemmeth F, Harlow J W, Bestwick A J, Rashba E I, Flensberg K, Stwertka C H, Taychatanapat T, Watson S K and Marcus C M 2009 Relaxation and dephasing in a two-electron ^{13}C nanotube double quantum dot *Phys. Rev. Lett.* **102** 166802

[14] Pályi A and Burkard G 2009 Spin–valley blockade in carbon nanotube double quantum dots *Phys. Rev.* B **82** 155424

[15] Reynoso A A and Flensberg K 2011 Dephasing and hyperfine interaction in carbon nanotube double quantum dots: the clean limit *Phys. Rev.* B **84** 205449

[16] Reynoso A A and Flensberg K 2012 Dephasing and hyperfine interaction in carbon nanotubes double quantum dots: disordered case *Phys. Rev.* B **85** 195441

[17] Ando T, Fowler A B and Stern F 1982 Electronic properties of two-dimensional systems *Rev. Mod. Phys.* **54** 437

[18] Schäffler F 1997 High-mobility Si and Ge structures *Semicond. Sci. Technol.* **12** 1515

[19] Culcer D, Cywiński Ł, Li Q, Hu X and Das Sarma S 2009 Realizing singlet–triplet qubits in multivalley Si quantum dots *Phys. Rev.* B **80** 205302

[20] Maune B M *et al* 2012 Coherent singlet–triplet oscillations in a silicon-based double quantum dot *Nature* **481** 344

[21] Goswami S *et al* 2007 Controllable valley splitting in silicon quantum devices *Nature Phys.* **3** 41

[22] Saraiva A L, Calderón M J, Capaz R B, Hu X, Das Sarma S and Koiller B 2011 Intervalley coupling for interface-bound electrons in silicon: an effective mass study *Phys. Rev.* B **84** 155320

[23] Lim W H, Yang C H, Zwanenburg F A and Dzurak A S 2011 Spin filling of valley–orbit states in a silicon quantum dot *Nanotechnology* **22** 335704

[24] Yang C H, Lim W H, Lai N S, Morello A and Dzurak A S 2012 Orbital and valley state spectra of a one-electron silicon quantum dot probed via charge sensing arXiv:1204.0843
[25] Shayegan M, Karrai K, Shkolnikov Y P, Vakili K, De Poortere E P and Manus S 2003 Low-temperature, *in situ* tunable, uniaxial stress measurements in semiconductors using a piezoelectric actuator *Appl. Phys. Lett.* **83** 5235
[26] Shayegan M, De Poortere E P, Gunawan O, Shkolnikov Y P, Tutuc E and Vakili K 2006 Two-dimensional electrons occupying multiple valleys in AlAs *Phys. Status Solidi* b **243** 3629
[27] Eriksson M A, Friesen M, Coppersmith S N, Joynt R, Klein L J, Slinker K, Tahan C, Mooney P M, Chu J O and Koester S J 2004 Spin-based quantum dot quantum computing in silicon *Quantum Inf. Process.* **3** 133
[28] Rycerz A, Tworzydlo J and Beenakker C W J 2007 Valley filter and valley valve in graphene *Nature Phys.* **3** 172
[29] Recher P, Trauzettel B, Rycerz A, Ya Blanter M, Beenakker C W J and Morpurgo A F 2007 Aharonov–Bohm effect and broken valley degeneracy in graphene rings *Phys. Rev.* B **76** 235404
[30] Gunawan O, Habib B, De Poortere E P and Shayegan M 2006 Quantized conductance in an AlAs two-dimensional electron system quantum point contact *Phys. Rev.* B **74** 155436
[31] Gunawan O, Shkolnikov Y P, Vakili K, Gokmen T, De Poortere E P and Shayegan M 2006 Valley susceptibility of an interacting two-dimensional electron system *Phys. Rev. Lett.* **97** 186404
[32] Recher P, Nilsson J, Burkard G and Trauzettel B 2009 Bound states and magnetic field induced valley splitting in gate-tunable graphene quantum dots *Phys. Rev.* B **79** 085407
[33] Wu G Y, Lue N-Y and Chang L 2011 Graphene quantum dots for valley-based quantum computing: a feasibility study *Phys. Rev.* B **84** 195463
[34] Culcer D, Hu X and Das Sarma S 2010 Interface roughness, valley–orbit coupling and valley manipulation in quantum dots *Phys. Rev.* B **82** 205315
[35] Culcer D, Saraiva A L, Koiller B, Hu X and Das Sarma S 2012 Valley-based noise-resistant quantum computation using Si quantum dots *Phys. Rev. Lett.* **108** 126804
[36] Wu Y and Culcer D 2012 Coherent electrical rotations of valley states in Si quantum dots using the phase of the valley–orbit coupling *Phys. Rev.* B **86** 035321
[37] Burkard G and Imamoglu A 2006 Ultra-long-distance interaction between spin qubits *Phys. Rev.* B **74** 041307
[38] Choi M-S, López R and Aguado R 2005 SU(4) Kondo effect in carbon nanotubes *Phys. Rev. Lett.* **95** 067204
[39] Kuemmeth F, Ilani S, Ralph D C and McEuen P L 2008 Coupling of spin and orbital motion of electrons in carbon nanotubes *Nature* **452** 448
[40] DiVincenzo D P 1995 Two-bit gates are universal for quantum computation *Phys. Rev.* A **51** 1015
[41] Barenco A, Bennett C H, Cleve R, DiVincenzo D P, Margolus N, Shor P, Sleator T, Smolin J A and Weinfurter H 1995 Elementary gates for quantum computation *Phys. Rev.* A **52** 3457
[42] Pályi A and Burkard G 2011 Disorder-mediated electron valley resonance in carbon nanotube quantum dots *Phys. Rev. Lett.* **106** 086801
[43] Makhlin Yu 2002 Nonlocal properties of two-qubit gates and mixed states, and the optimization of quantum computations *Quantum Inf. Process.* **1** 243
[44] Hanson R and Burkard G 2007 Universal set of quantum gates for double-dot spin qubits with fixed interdot coupling *Phys. Rev. Lett.* **98** 050502
[45] Stepanenko D and Burkard G 2007 Quantum gates between capacitively coupled double quantum dot two-spin qubits *Phys. Rev.* B **75** 085324
[46] Feher G and Gere E A 1959 Electron spin resonance experiments on donors in silicon. II. Electron spin relaxation effects *Phys. Rev.* **114** 1245
[47] Tyryshkin A M *et al* 2012 Electron spin coherence exceeding seconds in high-purity silicon *Nature Mater.* **11** 143
[48] Witzel W M, Carroll M S, Morello A, Cywiński Ł and Das Sarma S 2010 Electron spin decoherence in isotope-enriched silicon *Phys. Rev. Lett.* **105** 187602

[49] Fischer J, Trauzettel B and Loss D 2009 Hyperfine interaction and electron-spin decoherence in graphene and carbon nanotube quantum dots *Phys. Rev.* B **80** 155401
[50] Pályi A and Burkard G 2009 Hyperfine-induced valley mixing and the spin–valley blockade in carbon-based quantum dots *Phys. Rev.* B **80** 201404
[51] Lansbergen G P, Rahman R, Verduijn J, Tettamanzi G C, Collaert N, Biesemans S, Klimeck G, Hollenberg L C L and Rogge S 2011 Lifetime-enhanced transport in silicon due to spin and valley blockade *Phys. Rev. Lett.* **107** 136602
[52] Burkard G, Loss D and DiVincenzo D P 1999 Coupled quantum dots as quantum gates *Phys. Rev.* B **59** 2070
[53] Jespersen T S, Grove K, Rasmussen Paaske J, Muraki K, Fujisawa T, Nygard J and Flensberg K 2011 Gate-dependent spin–orbit coupling in multielectron carbon nanotubes *Nature Phys.* **7** 348
[54] Zhang J, Vala J, Sastry S and Whaley K B 2003 Geometric theory of nonlocal two-qubit operations *Phys. Rev.* A **67** 042313
[55] Di Vincenzo D P, Bacon D, Kempe J, Burkard G and Whaley K B 2000 Universal quantum computation with the exchange interaction *Nature* **408** 339